

## Supporting Information

# Molecular separations with breathing metal-organic frameworks: Modelling packed bed adsorbers

Tom R.C. Van Assche, Gino V. Baron and Joeri F.M. Denayer

Department of Chemical Engineering, Vrije Universiteit Brussel, Pleinlaan 2, B-1050 Brussel, Belgium

## 1. Model

Two differentsimulation techniques were used:

- 1) a partial differential equation solver using a finite difference scheme (**PDE method**).
- 2) a Stop-Go based method with instantaneous equilibrium (**SGE method**).

### 1.1 PDE method

The partial differential equation (PDE) method relies on solving a system of partial differential equations, described here for a binary mixture of component A and B, diluted in an excess of inert carrier gas. The adsorption kinetics are described by linear driving force equations<sup>1</sup>.

$$\begin{aligned} \frac{\partial c_A}{\partial t} + \frac{(1-\varepsilon_b)}{\varepsilon_b} \rho_b \frac{\partial q_A}{\partial t} &= - \left( \frac{v_{\text{sup}}}{\varepsilon_b} \right) \frac{\partial c_A}{\partial x} + D_{ax} \frac{\partial^2 c_B}{\partial x^2} \\ \frac{\partial c_B}{\partial t} + \frac{(1-\varepsilon_b)}{\varepsilon_b} \rho_b \frac{\partial q_B}{\partial t} &= - \left( \frac{v_{\text{sup}}}{\varepsilon_b} \right) \frac{\partial c_B}{\partial x} + D_{ax} \frac{\partial^2 c_B}{\partial x^2} \end{aligned} \quad (\text{s.1-2})$$

$$\begin{aligned} \frac{\partial q_A}{\partial t} &= K_{LDF,A} (q_A^{eq} - q_A) \\ \frac{\partial q_B}{\partial t} &= K_{LDF,B} (q_B^{eq} - q_B) \end{aligned} \quad (\text{s.3-4})$$

- c: concentration of adsorbate in mobile fluid phase (mol/m<sup>3</sup>)  
q: concentration of adsorbate in stationary phase (mol/kg)  
ε<sub>b</sub>: bed porosity  
v<sub>sup</sub>: superficial fluid velocity (m/s)  
x: axial coordinate (m)  
t: time (s)  
ρ<sub>b</sub>: bed density (kg/m<sup>3</sup>)  
K<sub>LDF</sub>: linear driving force coefficient (1/s)

No pressure drop or velocity variation (diluted case) is considered. The components obey the ideal gas law.

$$c = \frac{p}{RT} \quad (\text{s.5})$$

These equations are completed with equations expressing adsorption equilibrium.

$$\begin{aligned} q_A^{eq} &= (1-s) \left[ \frac{q_{sat1,A} \cdot K_{1,A} \cdot p_A}{1 + K_{1,A} \cdot p_A + K_{1,B} \cdot p_B} \right] + (s) \left[ \frac{q_{sat2,A} \cdot K_{2,A} \cdot p_A}{1 + K_{2,A} \cdot p_A + K_{2,B} \cdot p_B} \right] \\ q_B^{eq} &= (1-s) \left[ \frac{q_{sat1,B} \cdot K_{1,B} \cdot p_B}{1 + K_{1,A} \cdot p_A + K_{1,B} \cdot p_B} \right] + (s) \left[ \frac{q_{sat2,B} \cdot K_{2,B} \cdot p_B}{1 + K_{2,A} \cdot p_A + K_{2,B} \cdot p_B} \right] \end{aligned} \quad (\text{s.6-7})$$

These equations acknowledge a multicomponent Langmuir type of equilibrium for both phase 1 and phase 2, of a material able to transition between both phases. It must be noted that other types of multicomponent models may be used in a similar manner.  $s$  represents the mass fraction of phase 2. The  $s$ -function may be used to transition between both phases by a suitable function varying between 0 and 1. In this work eq. s.8 is used.

$$s = \frac{\exp(w_A [p_A - P_{tr,A}]) + \exp(w_B [p_B - P_{tr,B}])}{1 + \exp(w_A [p_A - P_{tr,A}]) + \exp(w_B [p_B - P_{tr,B}])} \quad (\text{s.8})$$

$w$ : width factor ( $\text{Pa}^{-1}$ )

$P_{tr}$ : transition pressure (Pa)

The  $s$ -function holds all information on the phase transfer. The above equation expresses a rectangular shaped phase diagram (Fig. 3.A) where the adsorbent materials adopts phase 1 in desorbed state and transitions to phase 2 if  $p_A$  is increased above  $P_{tr,A}$  or  $p_B$  is increased above  $P_{tr,B}$ .

Other  $s$ -functions may be used as well to yield more complex phase diagrams (Fig. 3.B). For example:

$$s = \frac{\exp(w [p_{tot} - P_{tr}])}{1 + \exp(w [p_{tot} - P_{tr}])} \quad (\text{s.9-10})$$

$$p_{tot} = p_A + p_B$$

The total transition pressure  $P_{tr}$  can be described in function of the composition by a suitable function (fitted on experimental or OFAST<sup>2</sup> predicted data).

$$P_{tr} = P_{tr}(y_A) \approx a + b \cdot y_A + c \cdot y_A^2 + \dots \quad (\text{s.11-12})$$

$$y_A = \frac{p_A}{p_{tot}}$$

This alternative  $s$ -function triggers a change in  $s$  (*i.e.* phase 2 mass fraction) when the total pressure exceeds the transition pressure  $P_{tr}$ . The latter is calculated using a suitable function describing the experimental PCL.

The above equations assume the adsorption column to be operated isothermally. The model can be made non-isothermal by considering the energy balance over the column and making all variables from the isotherm model (including the  $s$ -function) temperature dependent. It must be noted that the above  $s$ -functions describe a phase diagram (phase 1 – phase 2). This phase diagram is valid at the given temperature and total pressure ( $p_A + p_B + p_{inert}$ ) for a diluted case.

The initial conditions are:

$$\forall x, t = 0 \quad \begin{array}{l} c_A = q_A = 0 \\ c_B = q_B = 0 \end{array} \quad (\text{s.13-14})$$

The adsorbed amounts are in equilibrium with the zero feed concentrations according to the adsorption equilibrium equations (eq s.6-7).

The used boundary conditions:

$$\begin{aligned} c_A &= \frac{P_{init,A}}{RT} \\ c_B &= \frac{P_{init,B}}{RT} \end{aligned} \quad \forall t, x = 0 \quad (\text{s.15-18})$$

$$\begin{aligned} \frac{\partial q_A}{\partial t} &= K_{LDF,A}(q_A^{eq} - q_A) \\ \frac{\partial q_B}{\partial t} &= K_{LDF,B}(q_B^{eq} - q_B) \\ \frac{\partial c_A}{\partial x} &= 0 \\ \frac{\partial c_B}{\partial x} &= 0 \end{aligned} \quad \forall t, x = L \quad (\text{s.19-22})$$

For a non-diluted case, the interstitial velocity was no longer considered a constant<sup>3</sup> and calculated during the breakthrough simulation. The total mass balance is solved simultaneously.

$$\frac{\partial (v_{sup} / \varepsilon_b)}{\partial x} (c_A + c_B) = \frac{(1 - \varepsilon_b)}{\varepsilon_b} \rho_b \left( \frac{\partial q_A}{\partial t} + \frac{\partial q_B}{\partial t} \right) \quad (\text{s.23})$$

The equations were solved using the Athena Visual Studio 14.0 package (AthenaVisual, Inc.), typically using 2000 and 300 discretization points in time and axial distance respectively. Simulations were performed on a 2.3 GHz computer.

## **1.2 SGE method**

The Stop-Go Equilibrium (SGE) method is based on the Stop-Go method by Chihara *et al.*<sup>4</sup> The method uses a double series of cells, one row representing the fluid phase of inert carrier with trace amount of adsorbates (diluted case) while the second row represents the concentration of the adsorbates in the adsorbed phase. This concept is shown in Figure S.1. The SGE is based on two consecutive steps. In the GO step the contents of the fluid phase cells is passed one cell forward. During the STOP step, the equilibrium between the fluid phase cell and adsorbed phase cell is calculated using the mass balance (initially with the phase 1 multicomponent Langmuir model). Accordingly, this method calculates an instantaneous equilibrium. After equilibrium, the final concentrations are checked with the phase diagram. The fluid concentrations and partial pressures are linked by an ideal gas law.

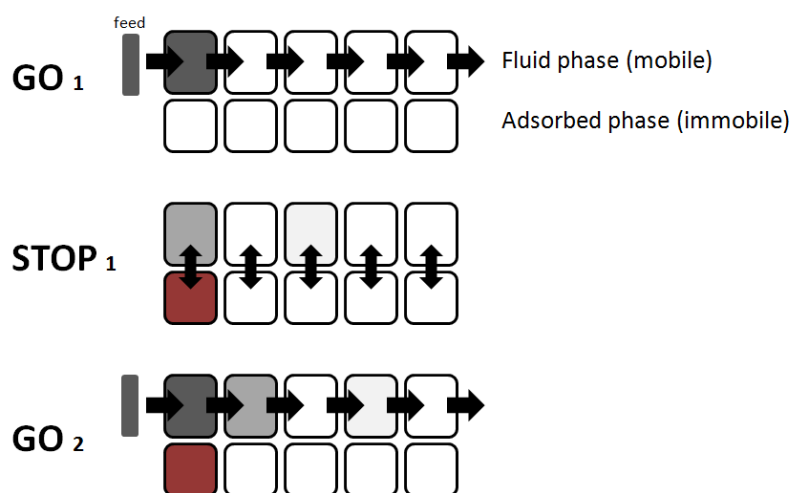


Figure S.1: Schematic representation of SGE method.

The phase diagram assumes a phase 1 to occur, unless  $p_A > P_{tr,A}$  or  $p_B > P_{tr,B}$ .

The SGE method is applied as a robust method capable of handling sudden shocks upon phase transition using conditional IF functions, rather than the smoothed equation s.8.

Expressed in this manner, the phase diagram resembles a rectangular phase diagram, as expressed by equation s.8 with the width factors  $w$  set very high. If the equilibrium concentrations calculated from the STOP step reveals these concentrations to lie in the phase 2 stability region, the calculation is repeated with the phase 2 multicomponent Langmuir model. Also this point is checked with the phase diagram.

Whenever  $p_A = P_{tr,A}$  or  $p_B = P_{tr,B}$ , a mixture of both adsorbent phases is allowed.

The initial concentration of the fluid and adsorbate phase was set at zero. This code is ran using Matlab R2012b (The Mathworks, Inc.) The calculations proceed by methodically solving systems of non-linear algebraic equations. Typical simulations involved 80 cells in series (distance) and up to 500 timesteps. Simulations were performed on a 2.3 GHz computer.

## 2. S-functions

The s-function of eq. s.8 can be used for a material which undergoes a single phase transition when the partial pressure of component A or B is increased. This basic equation can be modified to describe materials with multiple phase transitions (between two phases) or transitions between more than two phases. Some examples are given below.

### 1. One transformation: adsorbent with two phases

See eq. s.8, in combination with eq. s.6-7.

An example phase diagram is shown for  $w$  set high and  $P_{tr,A}$  and  $P_{br,B}$  set at 7 and 3 respectively. The blue zone corresponds to the stability region of phase 1, the red zone to the stability region of phase 2.

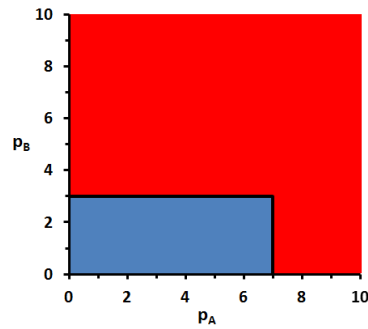


Figure S.2: Example of phase diagram by eq. s.8 (blue: phase 1, red: phase 2).

### 2. Two transformations: adsorbent with two phases

Eq. s.6-7 are now combined with a new s function.

$$s = s_{1to2} - s_{2to1}$$

$$s_{1to2} = \frac{\exp(w_{1A} [p_A - P_{tr1,A}]) + \exp(w_{1B} [p_B - P_{tr1,B}])}{1 + \exp(w_{1A} [p_A - P_{tr1,A}]) + \exp(w_{1B} [p_B - P_{tr1,B}])} \quad (\text{s.24-26})$$

$$s_{2to1} = \frac{\exp(w_{2A} [p_A - P_{tr2,A}]) + \exp(w_{2B} [p_B - P_{tr2,B}])}{1 + \exp(w_{2A} [p_A - P_{tr2,A}]) + \exp(w_{2B} [p_B - P_{tr2,B}])}$$

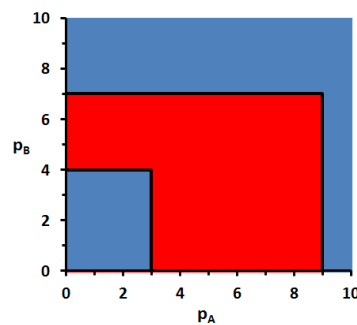


Figure S.3: Example of phase diagram by eq. s.24-26 (blue: phase 1, red: phase 2).

These equations only hold when  $P_{tr1,A} < P_{tr2,A}$  and  $P_{tr1,B} < P_{tr2,B}$ . An example phase diagram is shown in Figure S.3 for  $w$  set high and  $P_{tr,A}$ ,  $P_{tr,1B}$ ,  $P_{tr,2A}$  and  $P_{tr,2B}$  set at 3, 4, 9 and 7 respectively. The blue zone corresponds to the stability region of phase 1, the red zone to the stability region of phase 2.

### 3. Two sequential transformations: adsorbent with three phases

Eq. s.6-7, developed for a flexible adsorbent with two phases, must be adapted to describe a material transitioning between three phases. As an example, all phases are considered to have a multicomponent Langmuir behavior with adsorbates A and B.

(s.27-28)

$$q_A^{eq} = (1 - s_2 - s_3) \left[ \frac{q_{sat1,A} \cdot K_{1,A} \cdot p_A}{1 + K_{1,A} \cdot p_A + K_{1,B} \cdot p_B} \right] + (s_2) \left[ \frac{q_{sat2,A} \cdot K_{2,A} \cdot p_A}{1 + K_{2,A} \cdot p_A + K_{2,B} \cdot p_B} \right] + (s_3) \left[ \frac{q_{sat3,A} \cdot K_{3,A} \cdot p_A}{1 + K_{3,A} \cdot p_A + K_{3,B} \cdot p_B} \right]$$

$$q_B^{eq} = (1 - s_2 - s_3) \left[ \frac{q_{sat1,B} \cdot K_{1,B} \cdot p_B}{1 + K_{1,A} \cdot p_A + K_{1,B} \cdot p_B} \right] + (s_2) \left[ \frac{q_{sat2,B} \cdot K_{2,B} \cdot p_B}{1 + K_{2,A} \cdot p_A + K_{2,B} \cdot p_B} \right] + (s_3) \left[ \frac{q_{sat3,B} \cdot K_{3,B} \cdot p_B}{1 + K_{3,A} \cdot p_A + K_{3,B} \cdot p_B} \right]$$

In total, three phases are present and accordingly two  $s$ -functions are required to describe all the mass fractions of these phases. Function  $s_2$  describes the mass fraction of phase 2, while  $s_3$  describes the fraction of phase 3. An example of a set of  $s$ -functions is:

$$s_2 = s_{1to2} - s_{2to3}$$

$$s_3 = s_{2to3}$$

$$s_{1to2} = \frac{\exp(w_{1A} [p_A - P_{tr1,A}]) + \exp(w_{1B} [p_B - P_{tr1,B}])}{1 + \exp(w_{1A} [p_A - P_{tr1,A}]) + \exp(w_{1B} [p_B - P_{tr1,B}])} \quad (\text{s.29-32})$$

$$s_{2to3} = \frac{\exp(w_{2A} [p_A - P_{tr2,A}]) + \exp(w_{2B} [p_B - P_{tr2,B}])}{1 + \exp(w_{2A} [p_A - P_{tr2,A}]) + \exp(w_{2B} [p_B - P_{tr2,B}])}$$

These equations only hold when  $P_{tr1,A} < P_{tr2,A}$  and  $P_{tr1,B} < P_{tr2,B}$ . An example phase diagram is shown for  $w$  set high and  $P_{tr,A}$ ,  $P_{tr,1B}$ ,  $P_{tr,2A}$  and  $P_{tr,2B}$  set at 3, 2, 7 and 8 respectively. The blue zone corresponds to the stability region of phase 1, the red zone to the stability region of phase 2 and the green zone to the stability region of phase 3.

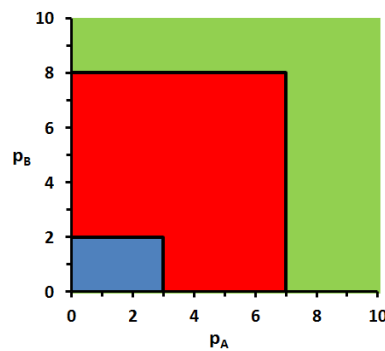


Figure S.4: Example of phase diagram by eq. s.29-32 (blue: phase 1, red: phase 2, green: phase 3).

### 3. Simulations for *ortho*-xylene/ethylbenzene separation on MIL-53(Al)

The experimental *ortho*-xylene and ethylbenzene breakthrough results of Finsy *et al.*<sup>5</sup> were simulated. The results of a simpler model, with a single rectangular shaped phase diagram as in Figure S.2, are shown in Figure 10 of the manuscript. This model acknowledges a single *narrow pore (np)* to *large pore (lp)* phase transformation. In this case, the material is in the *np* phase when fully desorbed.

A more rigorous model acknowledges two consecutive *lp-np* and *np-lp* transformations. In this case the material is in the *lp* phase when fully desorbed. This more rigorous model uses the parameters described in Table 1, as well as parameters for the initial *lp-np* transition: these are given in Table S.1. This model uses the *s*-function described by eq. s.24-26. Accordingly, the phase diagram has a shape similar to Figure S.3.

**Table S.1: Isotherm fitting parameters (eq. s.24-26, and used in eq. s.6-7) for pure component *ortho*-xylene (oX) and ethylbenzene (EB) adsorption on MIL-53(Al) at 383 K.**

|                               | oX     | EB     |
|-------------------------------|--------|--------|
| $K_{np}$ ( $\text{Pa}^{-1}$ ) | 0.56   | 0.56   |
| $q_{\text{sat},np}$ (mol/kg)  | 1.75   | 1.75   |
| $K_{lp}$ ( $\text{Pa}^{-1}$ ) | 0.0220 | 0.0035 |
| $q_{\text{sat},lp}$ (mol/kg)  | 4.0    | 4.0    |
| $P_{\text{tr}1}$ (Pa)         | 2      | 2      |
| $w_1$ ( $\text{Pa}^{-1}$ )    | 2      | 2      |
| $P_{\text{tr}2}$ (Pa)         | 200    | 6900   |
| $w_2$ ( $\text{Pa}^{-1}$ )    | 0.045  | 0.045  |

Figure S.5 shows the phase diagram (in logarithmic scale) of the above isotherm model.

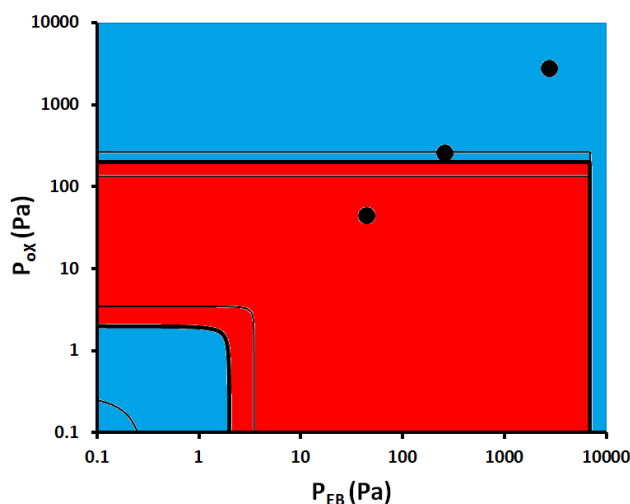


**Figure S.5: Phase diagram according to eq. s.24-26 and Table S.1 (logarithmic scale). The blue zones indicate a majority of *lp* to be present, the red zones a majority of *np* phase to be present. Thick lines indicate where a mixture 50/50 of *np/lp* phases exist. Thinner lines indicate a 95/5 or 5/95 mixture of phases. The black dots indicate the three feed points of Figure 10 and Figure S.6.**



The simulations of Figure 10 in the manuscript are repeated using this more rigorous model. The results are shown in Figure S.6. For the  $\sim 90$  Pa total hydrocarbon pressure simulation (Fig. S.9 A) a single  $lp$ - $np$  phase transition can be noticed. For the  $\sim 520$  Pa total hydrocarbon pressure simulation (Fig. S.9 B), an initial  $lp$ - $np$  contraction occurs followed by the gradual expansion of  $\sim 27$  wt.% of the crystals to  $lp$  phase. After this, the adsorbate rapidly adopts (almost) a full  $lp$  state. For the  $\sim 5600$  Pa total hydrocarbon pressure simulation (Fig. S.9 C), an initial  $lp$ - $np$  contraction occurs followed by the gradual expansion of only  $\sim 5$  wt.% of the crystals to  $lp$  phase. After this, the adsorbate rapidly adopts a full  $lp$  state. (Due to the relatively small width factors  $w$  of the first  $lp$ - $np$  contraction the fully desorbed state contains a small fraction of  $np$  phase.)

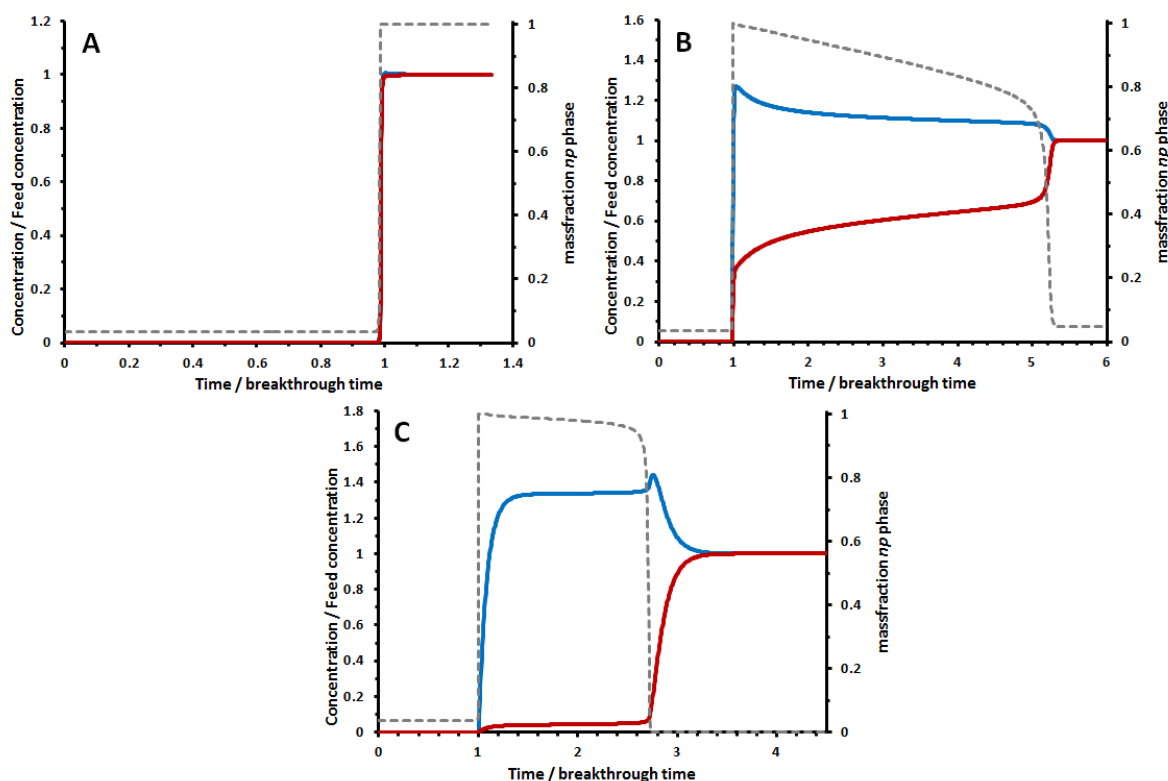


**Figure S.6: PDE simulated breakthrough results of equimolar mixture of *ortho*-xylene and ethylbenzene on MIL-53(Al), including the calculated fraction  $np$  phase (dashed gray line). Red: orthoxylene, Blue: ethylbenzene. Experiments with a total hydrocarbon pressure of (A) 90, (B) 520 and 5600 Pa are shown. In contrast to Figure 10, the  $s$ -function described by eq. s.24-26 was used in these simulations.**

- 1 B. Y. E. Glueckauf, in *Handbook of Ion Chromatography*, Wiley-VCH Verlag GmbH, Weinheim, Germany, 1955, vol. 51, pp. 13–25.
- 2 F.-X. Coudert, *Phys. Chem. Chem. Phys.*, 2010, **12**, 10904.
- 3 D.M. Ruthven, *Principles of adsorption & Adsorption processes*, John Wiley & Sons, 1984.
- 4 K. Chihara, I. Yoneda, S. Morishita and M. Suzuki, in *Studies in Surface Science and Catalysis*, Kodansha Ltd., 1986, vol. 28, pp. 563–570.
- 5 V. Finsy, C. E. A. Kirschhock, G. Vedts, M. Maes, L. Alaerts, D. E. De Vos, G. V. Baron and J. F. M. Denayer, *Chem. - A Eur. J.*, 2009, **15**, 7724–7731.